Ionic Liquids

DOI: 10.1002/anie.201102698

Crystalline Open-Framework Selenidostannates Synthesized in Ionic Liquids**

*Jian-Rong Li, Zai-Lai Xie, Xiao-Wu He, Long-Hua Li, and Xiao-Ying Huang**

Ionic liquids (ILs) receive ever growing attention owing to their ability to be an alternative of conventional organic solvents in many processes, as well as other fascinating applications.[1] The preparation of advanced functional materials making use of ILs, in particular ionothermal synthesis, has been shown to be very promising.[2] As such, the benefits of using ILs in materials synthesis have been put forward and discussed extensively.[3] However, such applications for chalcogenide chemistry is still in an early stage. To date most of the chalcogenides prepared in ILs are nanomaterials of known binaries.[4] Though recently there were reports of new crystalline chalcogenides obtained in ILs containing Lewis acids or strong acceptors, for example, EmimBr-$AlCl_3$,[5] the resulting products were limited to compounds featuring discrete clusters[5a–c] or cationic two-dimensional (2D) layer structure.[5d]

Crystalline microporous chalcogenides are desirable for applications such as ion exchange,[6] photocatalysis,[7] and fast ion conductivity.[8] Normally such materials contain an anionic framework with organic amine or alkali (or alkaline-earth) metal cations as the structure-directing agent (SDA) and charge compensating agent, and are synthesized by solvothermal or solid-state reactions.[9] Our aim is to develop a general preparative route in ILs for crystalline microporous chalcogenides with anionic three-dimensional (3D) or 2D structures. It is anticipated that the unique solvent properties of ILs and the structure-directing effect of their cations (e.g. imidazolium cations) would favor the formation of novel microporous chalcogenides that are inaccessible using traditional SDAs and traditional synthetic routes. However, our initial ionothermal reaction trials using imidazolium-based ILs always led to known binary chalcogenides or poor-crystalline powders/gels.

Hydrazine and hydrazine monohydrate ($N_2H_4{\cdot}H_2O$) have unique solvent properties, and have recently been widely used as efficient solvents or co-solvents in the synthesis and crystallization of inorganic solids, especially for chalcogenides.[10] We thought that the addition of a small quantity of $N_2H_4{\cdot}H_2O$ to an IL may change the solvent properties of the IL, and thus promote crystal growth. To explore the feasibility of this strategy, we chose selenidostannates as a model system, imidazolium chlorides as reactive ILs, and $N_2H_4{\cdot}H_2O$ as the auxiliary solvent. By changing the varieties of ILs and adjusting the weight fraction of IL and $N_2H_4{\cdot}H_2O$, four open-framework selenidostannates (see Scheme 1) with high crystallinity have been obtained, namely 3D-$[bmim]_4[Sn_9Se_{20}]$ (**1**) (bmim = 1-butyl-3-methyl imidazolium), 3D-$[bmmim]_4[Sn_9Se_{19}(Se_2)_{0.9}Se_{0.1}]$ (**2**) (bmmim = 1-butyl-2,3-dimethyl imidazolium), 3D-$[pmmim]_4[Sn_9Se_{19}(Se_2)_{0.93}Se_{0.07}]$ (**3**) (pmmim = 1-pentyl-2,3-dimethyl imidazolium), and 2D-$[pmmim]_8[Sn_{17}Se_{38}]$ (**4**). Compounds **1**–**3** represent the first examples of IL-directed 3D open-frameworks based on binary selenidostannates and compound **4** features 2D microporous structure composed of inorganic selenidostannate nanotubes.

The crystals of compound **1** were obtained by the reaction of tin, selenium, [bmim]Cl and $N_2H_4{\cdot}H_2O$ in a molar ratio of 1:2.5:5.7:8.0 at 160 °C for 5 days. Single-crystal X-ray diffraction analysis reveals that the structure of **1** features a 3D open-framework of anionic $[Sn_9Se_{20}]_n^{4n-}$ with multi-directional channels filled by $[bmim]^+$ cations, Figure 1. In the structure, the $[Sn_3Se_4]$ semicubes are linked together by two additional Se atoms that bridge one Sn atom from each cube to form $[Sn_6Se_{10}]$ units (Figure 1a), but which link to each other through $[SnSe_4]$ tetrahedra to form an infinite wavy chain running along the $[10\bar{1}]$ direction (Figure 1b). The chain further connects four adjacent such chains through $[Sn_2Se_6]$ units through corner-bridging to result in a 3D network.

Compound **2** was obtained in the reaction of tin, selenium, [bmmim]Cl, and $N_2H_4{\cdot}H_2O$ in a molar ratio of 1:2.5:5.3:1.6 at 160 °C for 5 days. Its structure features a 3D open-framework of $[Sn_9Se_{19}(Se_2)_{0.9}Se_{0.1}]_n^{4n-}$ with multi-directional channels filled by $[bmmim]^+$ cations, Figure 2. In the structure, the alternating $[SnSe_4]$ and $[SnSe_3(Se_2)_{0.9}Se_{0.1}]$ tetrahedra connect one $[Sn_3Se_4]$ semicube by corner-bridging and another $[Sn_3Se_4]$ semicube by edge-bridging, respectively, to form an infinite chain along the *a*-axis. Then two such chains are linked by $[SnSe_4]$ tetrahedra via corner-bridging to form a double-chain, Figure 2b. Each double-chain further connects four adjacent double-chains by edge-bridging the $[Sn_3Se_4]$ semicubes through two Se atoms, resulting in a 3D network.

Dark-red thin brick-like crystals of **3** accompanied by red rod-like crystals of **4** were obtained by the reaction of tin, selenium, [pmmim]Cl, and $N_2H_4{\cdot}H_2O$ in a molar ratio of 1:2.5:4.9:1.0 at 160 °C for 5 days. Simply by increasing the weight fraction of $N_2H_4{\cdot}H_2O$ to a 4.9:1.6 molar ratio of [pmmim]Cl:$N_2H_4{\cdot}H_2O$, pure phase of **4** could be obtained in a

[*] Dr. J.-R. Li, Z.-L. Xie, X.-W. He, Dr. L.-H. Li, Prof. X.-Y. Huang
State Key Laboratory of Structural Chemistry
Fujian Institute of Research on the Structure of Matter
Chinese Academy of Sciences
Fuzhou, Fujian 350002 (P. R. China)
E-mail: xyhuang@fjirsm.ac.cn

[**] This work was supported by the Knowledge Innovation Program of the Chinese Academy of Sciences (KJCX2-YW-H21), the NNSF of China (Grants 21001104, 07711022, and 20873149), and the NSF of Fujian Province (Grant 2008J0174). We thank Prof. Jian Zhang (FJIRSM) and Prof. Jing Li (Rutgers University) for the helpful discussions.

Supporting information for this article is available on the WWW under http://dx.doi.org/10.1002/anie.201102698.

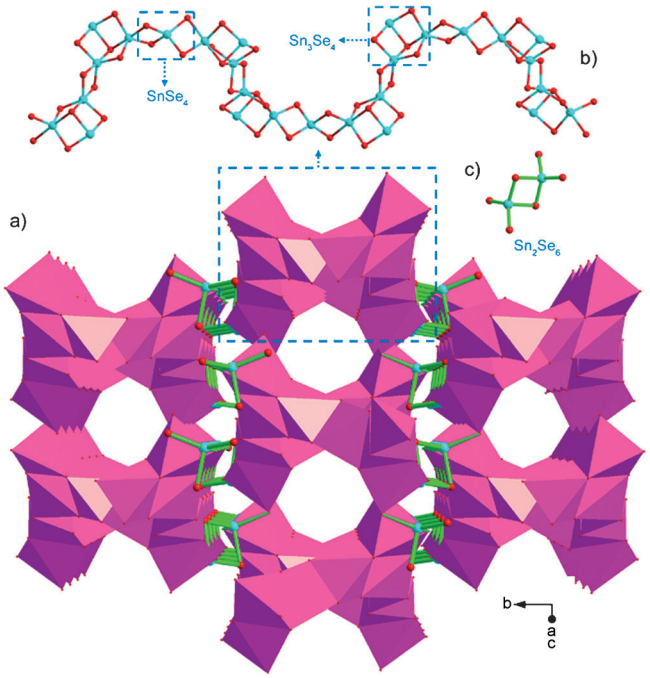

Figure 1. a) Polyhedral view of the anionic 3D framework in **1** along the $[10\bar{1}]$ direction. The Sn—Se bonds in the $[Sn_2Se_6]$ units are drawn in green. The $[bmim]^+$ in channels are omitted for clarity. b) An infinite $[Sn_7Se_{14}]$ chain in **1** running along the $[10\bar{1}]$ direction. c) The $[Sn_2Se_6]$ unit which connects four adjacent $[Sn_7Se_{14}]$ chains.

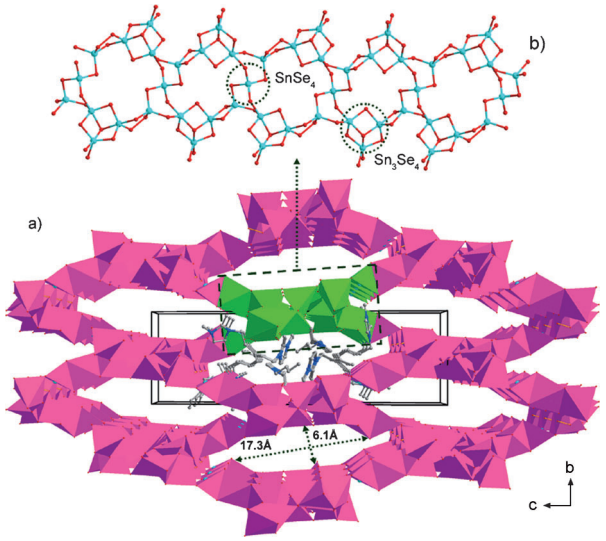

Figure 2. a) Polyhedral view of the structure of **2** along the *a*-axis. Most of the $[bmmim]^+$ (blue/gray stick models) in channels are omitted for clarity. b) View of the $[Sn_9Se_{17}(Se_2)_{0.9}Se_{0.1}]$ double-chain in **2** (highlighted in green in (a)) extended along the *a*-axis. The disordered $(Se_2)_{0.9}Se_{0.1}$ units are drawn as (Se_2) for clarity.

similar reaction. Compound **3** has an anionic 3D-$[Sn_9Se_{19}(Se_2)_{0.93}Se_{0.07}]_n^{4n-}$ open-framework similar to that of **2** except that its channels are filled with $[pmmim]^+$ cations. Calculation results show the interaction between anion and cation of **3** is stronger than that of **2**, and the binding energies also show that **3** is a little more stable than **2** (see Supporting Information). Compound **4** features a 2D $[Sn_{17}Se_{38}]_n^{4n-}$ layer parallel to the *ab* plane, Figure 3a. As illustrated in Figure 3b,c, there are two similar chains extended along the *a*-

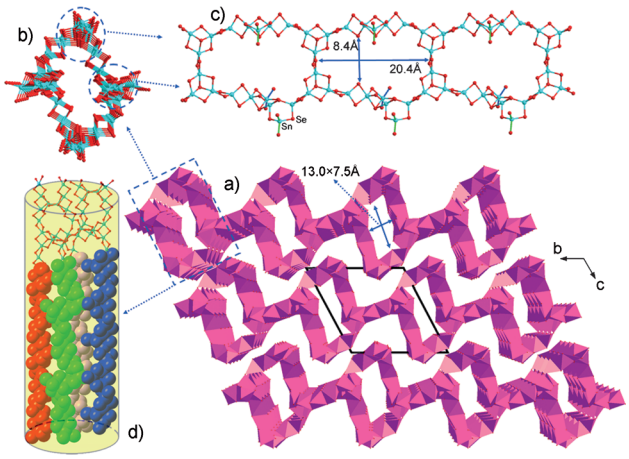

Figure 3. a) Polyhedral view of packing of the anionic layers of **4** along the *a*-axis. b) View of one nanotube in **4** along the *a*-axis. c) View of the double-chain comprising the nanotube. The Sn—Se bonds in the $[Sn_2Se_6]$ units are drawn in green. d) Schematic view of one nanotube along the [101] direction.

axis containing $[Sn_3Se_4]$ semicubes and $[SnSe_4]$ tetrahedra in different connection fashions, which are interlinked by edge-bridging the $[SnSe_4]$ tetrahedra of the respective $[Sn_3Se_4]$ semicubes from each chain to form a double-chain. Two such double-chains related by inversion centers are fused into a rectangle nanotube through bridging tetrahedral Sn atoms. The diameter of the nanotube is approximately 23.2 Å. The nanotubes further link to each other by edge-bridging the $[Sn_3Se_4]$ semicubes to form a layer extended along the *ab* plane. Therefore each layer consists of a series of 1D nanotubes arranged orderly with a cross-section of 13.0 × 7.5 Å. The layers further pack into 3D structure along the *c*-axis in *-AB-* fashion with the $[pmmim]^+$ cations filled in the nanotubes or interlayer spaces. Although some binary layered chalcogenides such as MS_2 (M = Mo, W) can form tubular structures,[11a,b] inorganic chalcogenide nanotubes are still scarce.[11c]

Remarkably, **1**–**3** all have nanopores in multi-directions. The largest cross-sections of the pore apertures are approximately 13.8 × 4.6 Å in **1** and 17.3 × 6.1 Å in **2**, respectively. All the structures are very open, evidenced by the large solvent-accessible volumes after excluding the cations (ca. 57.5%, 58.4%, 59.5%, and 64.4%, for **1**, **2**, **3** and **4**, respectively).[12] When the selenidostannate polyhedra are treated as nodes, the frameworks of **1** and **2** can be simplified into three (or four)-connected topologies with vertex symbols of (13)-$(3{\cdot}13{\cdot}14)_2(3{\cdot}13^2)_2(3^2{\cdot}13{\cdot}14^3)_2(3^2{\cdot}4{\cdot}13^2{\cdot}14)_2$ and $(3{\cdot}16^2)_2(3{\cdot}8{\cdot}9)_4$-$(3^2{\cdot}8{\cdot}9^2{\cdot}10)_2(3^2{\cdot}8^2{\cdot}9^2)$ (Figure 4), respectively, which have not been reported before. Note that the reported chalcogenidostannates are low dimensional structures in majority.[13] $A_2Sn_2Se_5$ (A = K, Rb) were the only examples of 3D selenidostannates.[14] This is probably due to the fact that fully connected 3D M^{4+}-Q (Q = S, Se) networks are neutral or

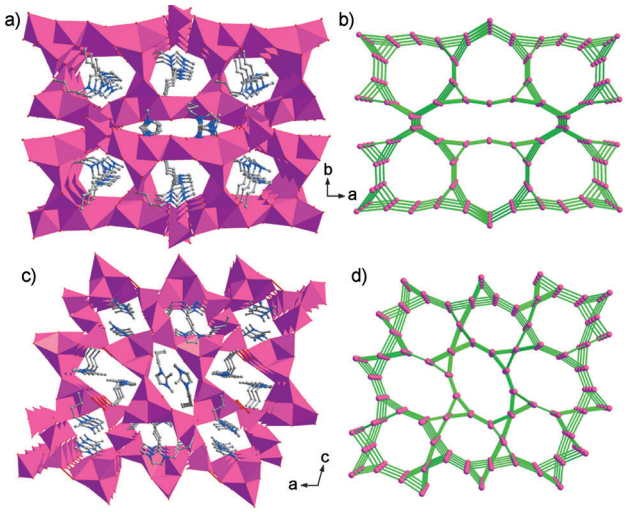

Figure 4. a) Polyhedral view of **1** along the *c*-axis. b) 3D framework topology of **1**. c) Polyhedral view of **2** along the *b*-axis. d) 3D framework topology of **2**. $[bmmim]^+$ blue/gray stick models.

low-valent anionic frameworks, making it difficult to find an effective SDA due to weak host–guest electrostatic interaction.[9a] Herein we have shown that the imidazolium cations are good SDAs for synthesizing open-framework selenidostannates that are not easily obtained using common SDAs.

To explore the optimal synthetic conditions, a series of reactions in the mixed solvents with a variety of weight fraction ratios of IL over $N_2H_4{\cdot}H_2O$ has been carried out (Scheme 1 and Supporting Information, Table S1). The reaction of Sn with Se in [bmim]Cl under ionothermal conditions ([bmim]Cl:$N_2H_4{\cdot}H_2O$ = 1:0, molar ratio) produced a black powder of $SnSe_2$. Whereas the similar ionothermal reactions by replacing [bmim]Cl by 1,2,3-trialkylimidazolium-based ILs ([bmmim]Cl and [pmmim]Cl) resulted in homogeneous red gels (Figure 5a,b). Solid products obtained from the red gels after washing by water and ethanol, namely **2**-NPs (NPs = nanoparticles) for [bmmim]Cl and **3**-NPs for [pmmim]Cl, were similar to **2** and **3** in chemical composition, respectively, as shown by powder X-ray diffraction (PXRD), elemental analysis, and thermogravimetric analysis (TGA). Scanning electronic microscope and transmission electron microscope

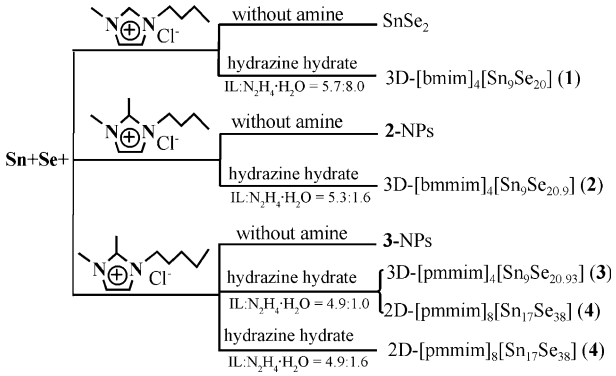

Scheme 1. Typical crystallization processes of new selenidostannates in ILs.

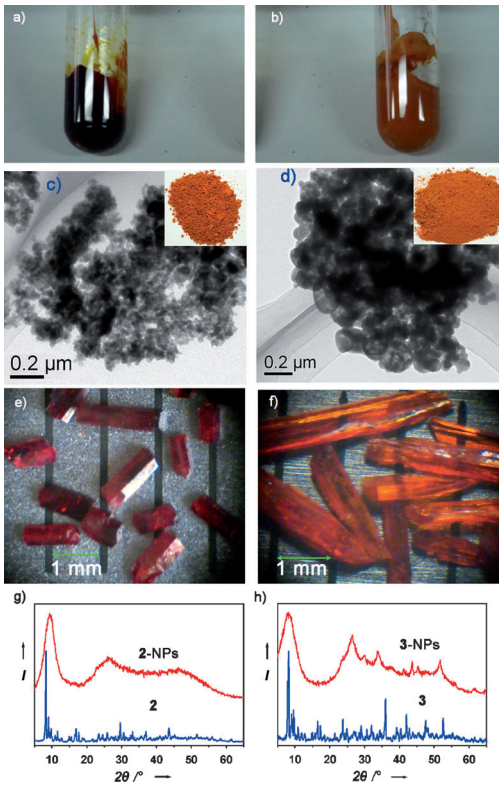

Figure 5. Photographs of the red gels obtained at ionothermal conditions (IL:$N_2H_4{\cdot}H_2O$ = 1:0, molar ratio) for IL = [bmmim]Cl (a) and IL = [pmmim]Cl (b). TEM images and photographs (inset) of the powders of **2**-NPs (c) and **3**-NPs (d) extracted from the respective red gels. Photographs of the crystals of **2** (e) and **4** (f) synthesized in IL:$N_2H_4{\cdot}H_2O$ = 5.3:1.6 and 4.9:1.6, respectively. Comparison of the PXRD patterns of **2** and **2**-NPs (g), and **3** and **3**-NPs (h).

(TEM) examinations indicated that **2**-NPs and **3**-NPs were aggregated to particles with average diameter of approximately 800 nm (Figure 5c,d and Supporting Information, Figure S3). Clearly new selenidostannate phases have formed under ionothermal conditions when using 1,2,3-trialkylimidazolium-based ILs as solvents (Figure 5g,h). However, it was likely the ILs as single solvent were still not suitable for further crystal growth, therefore only nanoparticles of **2** and **3** formed. In fact, the crystals of **1**–**4** formed well when a small amount of $N_2H_4{\cdot}H_2O$ was added. For instance, the sizes of the largest crystals of **2** and **4** are up to 1 mm (Figure 5e,f). The optimal crystallization conditions for **1**–**4** are illustrated in Scheme 1.

Interestingly, further increasing the weight fraction ratio of $N_2H_4{\cdot}H_2O$ over ILs led to different phenomena for various ILs (Supporting Information, Table S1). For instance, the major product was still **1** for [bmim]Cl when the molar ratio of [bmim]Cl:$N_2H_4{\cdot}H_2O$ was 2:15, whereas reactions with similar molar ratios of IL:$N_2H_4{\cdot}H_2O$ (IL = [bmmim]Cl or [pmmim]Cl) resulted in major products with well known 6^3 net $[Sn_3Se_7]_n^{2n-}$ layers intercalated by IL cations.[15]

Based on these results, it is clear that the selection of a suitable IL was important to the formation of open-framework selenidostannates and tuning of the crystal structures, further demonstrating the SDA effect of imidazolium cat-

ions.[16] The different performance of 1,3-dialkylimidazolium based ILs ([bmim]Cl) and 1,2,3-trialkylimidazolium based ILs as SDA and solvent may be ascribed to their different physicochemical properties, for example, polarity and acidity,[17a,b] and the ability of forming hydrogen bonds.[17c] The substitution of hydrogen in [bmim]Cl by a methyl group in [bmmim]Cl at the 2-positon of the imidazolium ring may hinder the hydrogen-bonding interaction with auxiliary solvent and selenidostannate framework.[17c] Thus it is assumed that [bmim]Cl is a stronger SDA than [bmmim]Cl, confirmed by the fact that a reaction using mixed [bmim]Cl and [bmmim]Cl in a molar ratio of 1:3.7 instead of individual ILs yielded the framework of **1** instead of **2** (Supporting Information, Table S1). As for [bmmim]Cl and [pmmim]Cl, the solvent properties such as viscosity and melting point vary with the length of alkyl chain, which also could exert great influence on the structure-directing effect and crystallization process, leading to the structure difference of **2** and **4**.

On the other hand, addition of $N_2H_4{\cdot}H_2O$ as an auxiliary solvent was a key factor in the formation of novel crystalline selenidostannates. $N_2H_4{\cdot}H_2O$, as the additive, may affect the properties of the mixed solvent (e.g. basicity), thus promoting the phase selectivity, crystallization process, and the yield of the crystalline products,[18] as has been observed in some solvothermal reactions in mixed solvent systems.[10] However, it's worth to mention that the crystals of compounds **2**, **3**, and **4** were obtained in the mixed solvents of IL as the major component and $N_2H_4{\cdot}H_2O$ as a minor additive, which are less molecular and more ionic in character.

The optical absorption spectra of **1**, **2**, and **4** were measured by diffuse reflectance experiments, indicating the absorption edges of 2.0 for **1**, 2.1 for **2**, and 2.0 eV for **4**, respectively, consistent with their red color (Supporting Information, Figure S6). In comparison, the measured absorption edges are 2.2 eV for **2**-NPs and 2.3 eV for **3**-NPs, respectively, exhibiting a little blue shift owing to their smaller particle size.

In summary, we have demonstrated a new strategy for the preparation of crystalline chalcogenides in ionic liquids. In particular the small amount of $N_2H_4{\cdot}H_2O$ appears to lead to a well-controlled crystallization process of chalcogenides. The obtained selenidostannates (**1**–**3**) represent the first three-dimensional framework chalcogenides synthesized in ILs. The finding would be helpful for understanding and a deliberate exploitation of specific interactions between ILs and chalcogenides, thus sheds light on the devolopement of facile synthetic routes in ILs towards crystalline open-framwork chalcogenides inaccessible in common solvents.

Experimental Section

The synthesis procedures for **1**–**4** are identical. The mixture of tin, selenium, ILs, and $N_2H_4{\cdot}H_2O$ (80%) was sealed in a 20 mL Teflon-lined bomb and was kept at 160 °C for five days, which was then slowly cooled to room temperature. The product was washed with water and ethanol and then the crystals of **1**–**4** were isolated by filtration and air-dried. The yields were calculated based on Sn. The red thin brick-like crystals of **1** (0.202 g, 57% yield) were obtained from a reaction of Sn (1.0 mmol, 0.119 g), Se (2.5 mmol, 0.197 g), [bmim]Cl (5.7 mmol, 1.00 g) and $N_2H_4{\cdot}H_2O$ (8.0 mmol, 0.50 g). The red thin brick-like crystals of **2** (0.218 g, 59% yield) were obtained from a reaction of Sn (1.0 mmol, 0.119 g), Se (2.5 mmol, 0.197 g), [bmmim]Cl (5.3 mmol, 1.00 g) and $N_2H_4{\cdot}H_2O$ (1.6 mmol, 0.10 g). The dark-red thin brick-like crystals of **3** accompanied by red rod-like crystals of **4** were obtained by a reaction of Sn (1.0 mmol, 0.119 g), Se (2.5 mmol, 0.197 g), [pmmim]Cl (4.9 mmol, 1.00 g) and $N_2H_4{\cdot}H_2O$ (1.0 mmol, 0.064 g). The crystals of **3** and **4** could easily be separated by hand. The pure phase of **4** were obtained by a reaction of tin (1.0 mmol, 0.119 g), Se (2.5 mmol, 0.197 g), (4.9 mmol, 1.00 g) and $N_2H_4{\cdot}H_2O$ (1.6 mmol, 0.10 g) (0.177 g, 47% yield).

Crystal Data for **1**: $C_{32}H_{60}N_8Se_{20}Sn_9$, $M_r = 3204.29$, monoclinic, Cc, $a = 19.974(8)$, $b = 26.854(10)$, $c = 14.575(6)$ Å, $\beta = 105.071(7)°$, $V = 7549(5)$ Å^3, $Z = 4$. $\rho_{calcd} = 2.819$ g cm^{-3}, $F(000) = 5752$, $\mu = 12.598$ mm^{-1}, $2.14° \le \theta \le 27.51°$, $T = 293(2)$ K, No. of reflections (measured/unique) = 29484/15056, $R_{int} = 0.051$, 11766 observed reflections $[I > 2\sigma(I)]$ with $R1(wR2) = 0.053$ (0.097), $R1(wR2) = 0.070$ (0.106) (all data), $GOF = 1.07$.

Crystal Data for **2**: $C_{36}H_{68}N_8Se_{20.9}Sn_9$, $M_r = 3331.46$, monoclinic, $P2_1/c$, $a = 20.594(5)$, $b = 11.083(2)$, $c = 36.208(8)$ Å, $\beta = 104.936(4)°$, $V = 7985(3)$ Å^3, $Z = 4$. $\rho_{calcd} = 2.771$ g cm^{-3}, $F(000) = 6002$, $\mu = 12.323$ mm^{-1}, $2.05° \le \theta \le 27.48°$, $T = 293(2)$ K, No. of reflections (measured/unique) = 59355/18280, $R_{int} = 0.040$, 14197 observed reflections $[I > 2\sigma(I)]$ with $R1(wR2) = 0.055$ (0.143), $R1(wR2) = 0.075$ (0.160) (all data), $GOF = 1.07$.

Crystal Data for **3**: $C_{40}H_{76}N_8Se_{20.93}Sn_9$, $M_r = 3389.93$, monoclinic, $P2_1/c$, $a = 20.3576(4)$, $b = 11.6146(3)$, $c = 36.0552(6)$ Å, $\beta = 105.054(2)°$, $V = 8232.5(3)$ Å^3, $Z = 4$. $\rho_{calcd} = 2.735$ g cm^{-3}, $F(000) = 6134$, $\mu = 11.968$ mm^{-1}, $2.48° \le \theta \le 26.55°$, $T = 293(2)$ K, No. of reflections (measured/unique) = 35987/17059, $R_{int} = 0.034$, 10158 observed reflections $[I > 2\sigma(I)]$ with $R1(wR2) = 0.032$ (0.047), $R1(wR2) = 0.067$ (0.048) (all data), $GOF = 1.03$.

Crystal Data for **4**: $C_{80}H_{152}N_{16}Se_{38}Sn_{17}$, $M_r = 6356.40$, triclinic, $P\bar{1}$, $a = 20.351(10)$, $b = 21.901(11)$, $c = 22.832(12)$ Å, $\alpha = 113.678(5)$, $\beta = 110.831(7)$, $\gamma = 93.216(10)°$, $V = 8472(7)$ Å^3, $Z = 2$. $\rho_{calcd} = 2.492$ g cm^{-3}, $F(000) = 5772$, $\mu = 10.656$ mm^{-1}, $2.01° \le \theta \le 27.46°$, $T = 130$ K, No. of reflections (measured/unique) = 56755/31978, $R_{int} = 0.052$, 17383 observed reflections $[I > 2\sigma(I)]$ with $R1(wR2) = 0.063$ (0.151), $R1(wR2) = 0.093$ (0.166) (all data). $GOF = 1.02$.

CCDC 821042 (**1**), 821043 (**2**), 821044 (**3**) and 821045 (**4**) contain the supplementary crystallographic data for this paper. These data can be obtained free of charge from The Cambridge Crystallographic Data Centre via www.ccdc.cam.ac.uk/data_request/cif.

Received: April 19, 2011
Revised: June 17, 2011
Published online: October 10, 2011

Keywords: chalcogenides · ionic liquids · open-framework structures · selenium · tin

[1] R. D. Rogers, K. R. Seddon, *Science* **2003**, *302*, 792–793.
[2] a) R. E. Morris, *Chem. Commun.* **2009**, 2990–2998; b) E. R. Parnham, R. E. Morris, *Acc. Chem. Res.* **2007**, *40*, 1005–1013; c) E. R. Cooper, C. D. Andrews, P. S. Wheatley, P. B. Webb, P. Wormald, R. E. Morris, *Nature* **2004**, *430*, 1012–1016.
[3] a) Z. Ma, J. H. Yu, S. Dai, *Adv. Mater.* **2010**, *22*, 261–285; b) A. Taubert, Z. Li, *Dalton Trans.* **2007**, 723–727.
[4] a) X. D. Liu, J. M. Ma, P. Peng, W. J. Meng, *Langmuir* **2010**, *26*, 9968–9973; b) K. Biswas, C. N. R. Rao, *Chem. Eur. J.* **2007**, *13*, 6123–6129; c) J. Jiang, S. H. Yu, W. T. Yao, H. Ge, G. Z. Zhang, *Chem. Mater.* **2005**, *17*, 6094–6100; d) Y. Jiang, Y. J. Zhu, *J. Phys. Chem. B* **2005**, *109*, 4361–4364.
[5] a) D. Freudenmann, C. Feldmann, *Dalton Trans.* **2011**, *40*, 452–456; b) Q. Zhang, I. Chung, J. I. Jang, J. B. Ketterson, M. G. Kanatzidis, *J. Am. Chem. Soc.* **2009**, *131*, 9896–9897; c) H. Sakamoto, Y. Watanabe, T. Saito, *Inorg. Chem.* **2006**, *45*, 7028–

7028; d) K. Biswas, Q. C. Zhang, I. Chung, J. H. Song, J. Androulakis, A. J. Freeman, M. G. Kanatzidis, *J. Am. Chem. Soc.* **2010**, *132*, 14760 – 14762.
[6] M. J. Manos, K. Chrissafis, M. G. Kanatzidis, *J. Am. Chem. Soc.* **2006**, *128*, 8875 – 8883.
[7] N. F. Zheng, X. H. Bu, H. Vu, P. Y. Feng, *Angew. Chem.* **2005**, *117*, 5433 – 5437; *Angew. Chem. Int. Ed.* **2005**, *44*, 5299 – 5303.
[8] N. F. Zheng, X. H. Bu, P. Y. Feng, *Nature* **2003**, *426*, 428 – 432.
[9] a) P. Y. Feng, X. H. Bu, N. F. Zheng, *Acc. Chem. Res.* **2005**, *38*, 293 – 303; b) S. Dhingra, M. G. Kanatzidis, *Science* **1992**, *258*, 1769 – 1772.
[10] a) H. Wiogo, M. Lim, P. Munroe, R. Amal, *Cryst. Growth Des.* **2011**, *11*, 1689 – 1696; b) Y. J. Dong, Q. Peng, Y. D. Li, *Inorg. Chem. Commun.* **2004**, *7*, 370 – 373; c) W. T. Yao, S. H. Yu, X. Y. Huang, J. Jiang, L. Q. Zhao, L. Pan, J. Li, *Adv. Mater.* **2005**, *17*, 2799 – 2807; d) M. Yuan, D. B. Mitzi, *Dalton Trans.* **2009**, 6078 – 6088; e) J. R. Li, X. Y. Huang, *Dalton Trans.* **2011**, *40*, 4387 – 4390.
[11] a) Y. Feldman, E. Wasserman, D. J. Srolovitz, R. Tenne, *Science* **1995**, *267*, 222 – 225; b) Y. D. Li, X. Li, R. He, J. Zhu, Z. Deng, *J. Am. Chem. Soc.* **2002**, *124*, 1411 – 1416; c) C. D. Malliakas, M. G. Kanatzidis, *J. Am. Chem. Soc.* **2006**, *128*, 6538 – 6539.
[12] A. L. Spek, *PLATON*, A Multipurpose Crystallographic Tool, Utrecht University, Utrecht, the Netherlands, **2010**.
[13] a) T. Jiang, G. A. Ozin, *J. Mater. Chem.* **1998**, *8*, 1099 – 1108; b) W. S. Sheldrick, M. Wachhold, *Coord. Chem. Rev.* **1998**, *176*, 211 – 322.
[14] a) K. O. Klepp, *Z. Naturforsch. B* **1992**, *47*, 197 – 200; b) W. S. Sheldrick, H. G. Braunbeck, *Z. Naturforsch. B* **1992**, *47*, 151 – 153.
[15] J.-R. Li, X.-Y. Huang, unpublished results.
[16] E. R. Parnham, R. E. Morris, *Chem. Mater.* **2006**, *18*, 4882 – 4887.
[17] a) Y. Yoshida, O. Baba, C. Larriba, G. Saito, *J. Phys. Chem. B* **2007**, *111*, 12204 – 12210; b) Y. J. Kim, A. Streitwieser, *J. Am. Chem. Soc.* **2002**, *124*, 5757 – 5761; c) P. A. Hunt, *J. Phys. Chem. B* **2007**, *111*, 4844 – 4853.
[18] a) L. Wang, Y. P. Xu, Y. Wei, J. C. Duan, A. B. Chen, B. C. Wang, H. J. Ma, Z. J. Tian, L. W. Lin, *J. Am. Chem. Soc.* **2006**, *128*, 7432 – 7433; b) R. S. Xu, W. P. Zhang, J. Guan, Y. P. Xu, L. Wang, H. J. Ma, Z. J. Tian, X. W. Han, L. W. Lin, X. H. Bao, *Chem. Eur. J.* **2009**, *15*, 5348 – 5354.

